SIZE AND COLOR DISTRIBUTIONS OF SMALL MAIN-BELT ASTEROIDS OBSERVED BY THE SUBARU/HYPER SUPRIME-CAM. Takuto Deyama[1], Tsuyoshi Terai[2], Keiji Ohtsuki[1] and Fumi Yoshida[3], [1]Department of Planetology, Kobe University, Kobe 657-8501, Japan; tdeyama@stu.kobe-u.ac.jp, [2]Subaru Telescope, National Astronomical Observatory of Japan, National Institutes of Natural Sciences, [3]Planetary Exploration Research Center, Chiba Institute of Technology.

Introduction: Size distributions of small-body populations provide important clues to the origin and evolution of the Solar System. Since the size distribution reflects collisional evolution of asteroids, we may be able to derive constraints on the dynamical history as well as material strength of asteroids from their current size distribution. Also, a better understanding of the evolution of the size distribution of asteroids is expected to improve our understanding of delivery of small bodies into the terrestrial regions. The main-belt asteroids are thought to be the major source of meteoroids and the near-Earth asteroids, and their size distribution is related to the production rates of these small bodies. Furthermore, some of the craters on the surface of the terrestrial planets and the moon were likely created by impacts of asteroids, while others would have been created by impacts of icy bodies that were transported from the outer Solar System [e.g., 1,2]. Thus, an improved knowledge of the size distribution of asteroids would help us better identify the source of impactors on these bodies. Recently, it has been suggested that comparison between size distributions of small bodies in different dynamical groups would provide us a unique constrain on the radial mixing of small bodies caused by giant planet during their migration [3]. In order to derive more useful constrains through comparison with theoretical modelling as well as observations of craters, a better understanding of the current size distribution of small asteroids is essentially important.

On the other hand, surface properties of small bodies also provide important constraints on their origin and evolution. Although spectroscopic studies of these bodies can provide us useful information about their surface properties and composition, it is difficult to obtain high-quality spectra for many objects. On the other hand, photometric observation using multiple broadband filters allows us to perform a statistical study of a large number of objects. Size and color distribution of small main-belt asteroids using the Suprime-Cam of the Subaru Telescope was carried out previously [4]. The study showed that the slopes of the size distributions of small main-belt asteroids would be different between the two color groups. It also examined the radial distribution of asteroids for each color group. However, more detailed studies with a larger sample is required to clarify the dependence of the size distribution and radial distribution on their surface properties.

In the present work, we examine size and color distribution of small main-belt asteroids observed by the Hyper Suprime-Cam (HSC) installed on the Subaru Telescope. The HSC is a prime focus camera for the 8.2m Subaru Telescope, and consists of 116 2048 × 4096 pixel CCDs (104 for science, 8 for focus monitoring, and 4 for auto guiding). It has a field of view (hereafter FOV) 1.5 degree in diameter with a pixel scale of 0.168 arcsec [5]. This wide FOV allows us to obtain a larger number of samples and improves statistical analysis of the size and color distributions of observed objects.

Methods: We use the data obtained with the HSC on January 25, 2015. The observation was carried out for nine FOVs with the *r*- and *g*-band filters. Each FOV was visited five times with each band. Here we report our preliminary results for one of these fields. The detection of moving objects was performed in the *r*-band observations, and 354 moving objects whose sky motion corresponds to that of main-belt asteroids were detected for the FOV we examined in the present work. After removing faint or vague objects, we did photometry for 306 objects that were detected with both *g*- and *r*-bands. We performed aperture photometry for these objects. The geocentric distances of these objects were calculated from apparent velocities, assuming that the objects were at opposition and their orbits are circular [6]. Then we convert their apparent magnitudes to absolute magnitudes using the derived geocentric distances. The *g*-*r* color of these objects was calculated from the difference in the *g*-band and *r*-band magnitudes.

Figure 1 shows the histogram of the *g*-*r* color distribution. Since we found a dip around $g\text{-}r = 0.4$ in this histogram, we divide the samples into two groups by this value. A similar grouping was done by the previous work [4]. Following this previous work, we call those asteroids with $g\text{-}r > 0.4$ "S-like asteroids", and those with $g\text{-}r < 0.4$ are called "C-like asteroids".

In order to obtain an unbiased size distribution of the detected asteroids, we have to set detection limits as follows. We analyzed only those objects with heliocentric distance equal to or smaller than 3.0 au, and *r*-band apparent magnitude equal to or smaller than 24. These limits were chosen because the number of our

detected objects decreases significantly beyond 3.0 au, and also because the detection efficiency drops abruptly at around 24 magnitude. The above two conditions lead the absolute magnitude limit to be 20.1 magnitude. After applying these restrictions, the number of the remaining sample was 169. Furthermore, we estimated the detection efficiency for each CCD by implanting pseudo moving objects into our corrected images, detecting these pseudo objects, and then comparing the number of implanted objects with that of the detected ones (see [7] for detail). Using the derived detection efficiency, we corrected the number of detected objects for each magnitude bin when obtaining magnitude distribution.

Results: We derived cumulative size distributions for the S-like and the C-like asteroids, using the obtained absolute magnitudes and assuming size-uncorrelated albedos. The numbers of objects are 106 and 63 for the S-like and the C-like asteroids, respectively. We fit an assumed power-law function $\Sigma(H) = 10^{\alpha(H-H0)}$ to each of the obtained distributions by the maximum-likelihood method and derived the values of α and H_0. We found that the values of α for the S-like and the C-like asteroids agree with each other within the fitting error, although the shapes of the curves are somewhat different. Figures 2 and 3 show the cumulative size distributions of the S-like and the C-like asteroids, respectively. Although the distribution for the C-like asteroids is well approximated by the fitting line, it seems that the distribution of the S-like asteroids would not be represented by a single power-law.

The difference in the cumulative size distributions of S-like and C-like asteroids may reflect their different impact strength law that depends on the bulk materials and/or internal structures. Such a difference in the slopes has been noted by the previous works based on the data obtained by the Subaru/Suprime-Cam [4] or the Sloan Digital Sky Survey [8]. Especially, the work using the Subaru/Suprime-Cam found a break in the fitting line for the S-like asteroids [4]. In present work, we fit the data with a single power-law, because the fitting accuracy is too low if we fit by multiple lines since the number of our sample is not sufficiently large. By adding data for the remaining eight FOVs, we expect to derive more accurate size distributions of small main-belt asteroids compared to the previous work [4].

Acknowledgements: This work was supported by JSPS KAKENHI Nos. 15H03716, 16H04041 (K.O.), 18K13607 (T.T.), and 16K05546 (F.Y.).

References: [1] Gomes R. S., et al. (2005) Nature, 435, 466. [2] Strom, R. G., et al. (2005) Science, 309, 1847. [3] Yoshida, F., et al. (2019) P&SS, in press. [4] Yoshida, F., & Nakamura, T. (2007) P&SS, 60, 297. [5] Miyazaki, S., et al. (2012) Proc. SPIE, 8446, 84460Z. [6] Jedicke, R. (1996) AJ, 111, 970. [7] Yoshida, F., & Terai, T. (2017) AJ, 154, 71. [8] Ivesić, Ž., et al. (2002) AJ, 122, 2749.

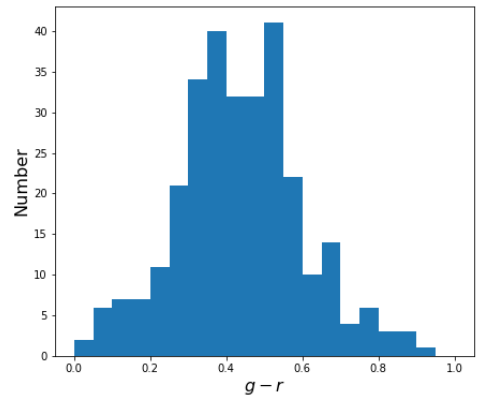

Figure 1: Histogram of the *g-r* color for the 306 objects examined in the present work.

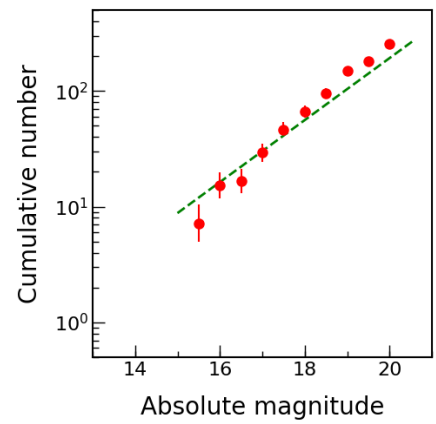

Figure 2: Cumulative size distribution of the S-like asteroids. Points show the number of objects for each magnitude bin, and the dashed line represents the best-fit power-law distribution.

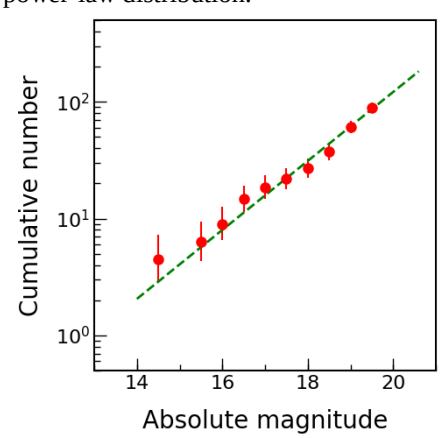

Figure 3: Same as Figure 2, but for the C-like asteroids.